ISSN 2007-9737

Wind Flow Analysis of Twisted Savonius Micro-Turbine Array

Jesús Antonio Alvarez-Cedillo, Mauricio Olguín-Carbajal, Juan Carlos Herrera-Lozada, Ramón Silva-Ortigoza, Jacobo Sandoval-Gutiérrez

Instituto Politécnico Nacional, Centro de Innovación y Desarrollo Tecnológico en Cómputo, Mexico City, Mexico

{jaalvarez, molguinc, jlozada, rsilvao}@ipn.mx, jacobosandoval@hotmail.com

Abstract. This paper provides a computational analysis of wind impact on different geometric configurations of Savonius turbines proposed and previously studied in specialized literature. As a result of comparative analysis of turbines, we performed a flow analysis over a micro-turbine array, proposed a twisted Savonius turbine respecting its original profile, and subjected it to a comparative analysis of its performance against conventional turbines. Our new proposal of Savonius turbines stands out due to its lower residual turbulence. The turbine dimensions are suited to the geometric relationships previously analyzed, and they are suggested in a way to respect the original profile of each turbine. The size of each turbine is small since its application is proposed for power generation in a low power array which can be placed on any building as part of its outer walls.

Keywords. Wind energy, Savonius turbine, low-power turbines, aerodynamics, fluid analysis.

1 Introduction

The wind industry is the most dynamic one among the largest industries producing equipment for power generation. Within the set of emerging industries it has been overtaken only by the mobile phone industry. Wind power generation has shown a tremendous growth over the past decade; it is recognized as a production of environmentally friendly energy and an economically competitive means for power generation [1].

A wind turbine is a device that converts the wind kinetic energy into rotational kinetic energy which is then turned into electrical energy. Wind turbines have the advantage of being modular and can be installed relatively quickly which makes them an attractive source of power generation compared to other types of alternative energies such as hydro-power energy. There are many different types of wind turbines, they can be divided into two large groups depending on rotation axis orientation of the turbine: wind turbines with horizontal axis and those with vertical axis [2, 3, 4, 5].

Turbines with vertical axis are most competitive due to such factors as the ability to capture the wind in any direction [6], their comparatively simple structure, easy maintenance, a low cost of implementation and installation. Among vertical axis wind turbines, there is the Savonius turbine, which was created by the Finnish engineer S. J. Savonius [7] in 1931 as a drag-type of the vertical axis wind turbine. The configuration for this turbine is a cross section in the form of an "S" built by two semicircular blocks with a small overlap. Its operating principle is based on the difference of drag forces between the convex and concave parts of the turbine [8]. This paper gives a computational analysis of the Savonius turbine flow with different geometric configurations [6, 9], observing the behavior of the air flow that strikes them, determining the best configuration for their application in modular systems mounted on buildings.

This paper is organized as follows. Section 2 describes the Savonius turbine geometric configuration. Section 3 introduces the three dimensional modeling of Savonius turbine and presents our proposal with the computational analysis of the wind flow over the Savonius turbine. In Section 4 the results are discussed. Finally, Section 5 presents our conclusions and future work.

ISSN 2007-9737

2 Geometric Configurations

Experimental [6, 8, 10, 11] and numerical [2, 3, 5, 9] studies on the geometric variables of a Savonius turbine were made in order to improve performance and make better use of wind power. However, even when the turbine profile is very different, the same power coefficient (C_p) has been reached, this coefficient is defined as

$$C_p = TSR * C_t , \quad (1)$$

where C_t is the torque coefficient (dimensionless, calculated on trial basis), and the TSR (Tip Speed Ratio) is defined as

$$TSR = (\omega * D) / U , \quad (2)$$

where
ω is the turbine angular velocity [rad/s],
D is the turbine diameter [m],
U is the wind speed [m/s].

Due to the fact that C_p is directly linked to the turbine maximum efficiency which depends on the energy amount able to draw air, the mechanical power (P_w) obtained by a wind turbine is expressed as

$$P_w = 1/2 * \rho * A * U^3 , \quad (3)$$

where
ρ is the air specific density (1,225 Kg/m^3), and A is the area that is swept by the turbine blades (m^2).

As Betz Limit indicates [18], no wind turbine can convert more than 59% of the wind kinetic energy into the mechanical energy turning a rotor. Today this is known as the Betz's Law and 59% is called the maximum power coefficient defined as

$$C_{\rho MAX} = 0.59.$$

In practice, wind turbines cannot operate at this maximum limit. The C_ρ value is unique for each type of wind turbine and depends on the wind speed that the turbine is operating and the turbine itself. In experimental research conducted by M. A. Kamoji et al. [4], a $C_{\rho MAX}$ of 0.21 was reached with the geometric relationships shown in Table 1. In this table:

- m represents the lag between the blades [m],
- H is the turbine height [m],
- ψ is the blade arc angle [°],
- p is the straight part of each blade [m],
- q is the blade arc radius [m],
- D_o is the plate diameter [m].

Table 1. Geometric relationships for a $C_{\rho MAX}$ [4]

m/D	*H/D*	*Ψ*	*p/q*	*Do/D*
0	0.7	124°	0.2	1.1

A two-dimensional image for this Savonius turbine profile without shaft is analyzed in [4] and shown in Fig. 1; a Savonius turbine with shaft is studied in [5] and shown in Fig. 2.

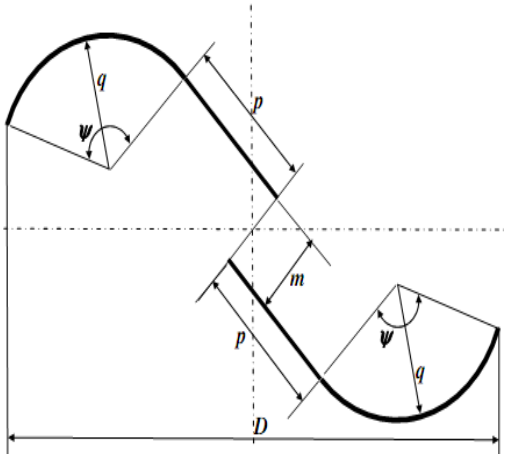

Fig. 1. Savonius turbine without shaft

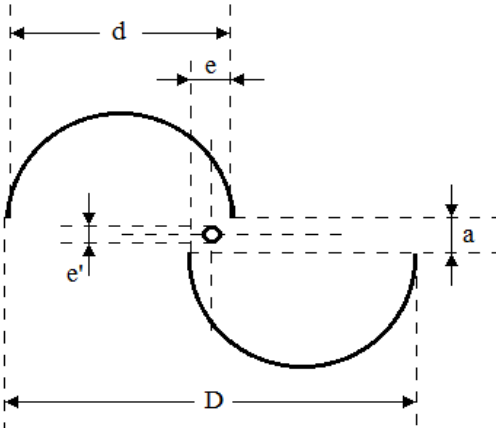

Fig. 2. Savonius turbine with shaft

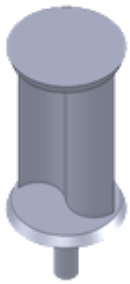

Fig. 3. 3D model of the Savonius turbine without shaft

Fig. 4. 3D model of the Savonius turbine with shaft

Fig. 5. 3D model of the twisted Savonius turbine

Furthermore, J-L Menet et al. [9] conducted a parametric investigation to increase the turbine efficiency with a different geometric configuration, in which it is possible to obtain a maximum C_t of 0.33 which is reflected in a maximum C_p of 0.3. This represents a 12% improvement in C_p. This different profile is shown in Fig. 2, while Table 2 shows the geometric relationships which are based on the work of Menet. In Table 2:

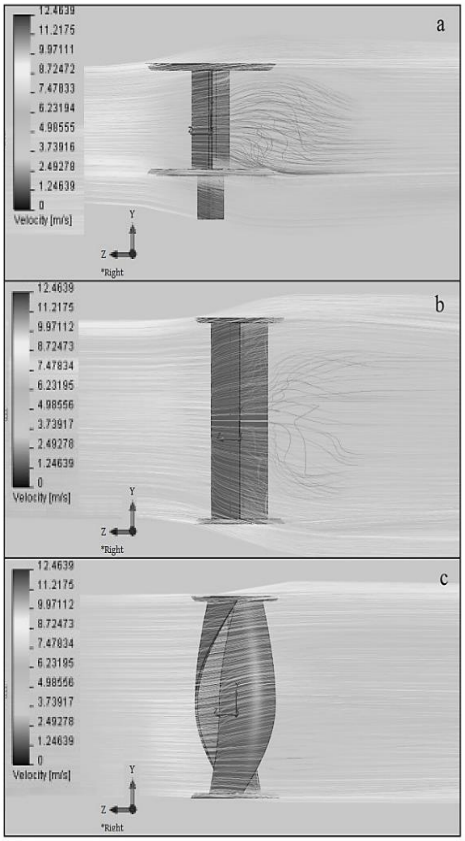

Fig. 6. Flow paths on the different 3D Savonius turbines

- d is the circle internal diameter formed by each blade [m],
- e is the distance between blades' overlap [m],
- e' is the shaft diameter [m].

Table 2. Geometric relationships to obtain C_{pMAX} [5]

m/D	*H/D*	*ψ*	*p/q*	*(e-e')/d*	*D_o/D*
0	2	180°	0	0.242	1.1

3 Three-Dimensional Modeling of Savonius Turbine

The profiles presented in Section 2 are modeled in 3D with SolidWorks software following the previously mentioned geometric relationships.

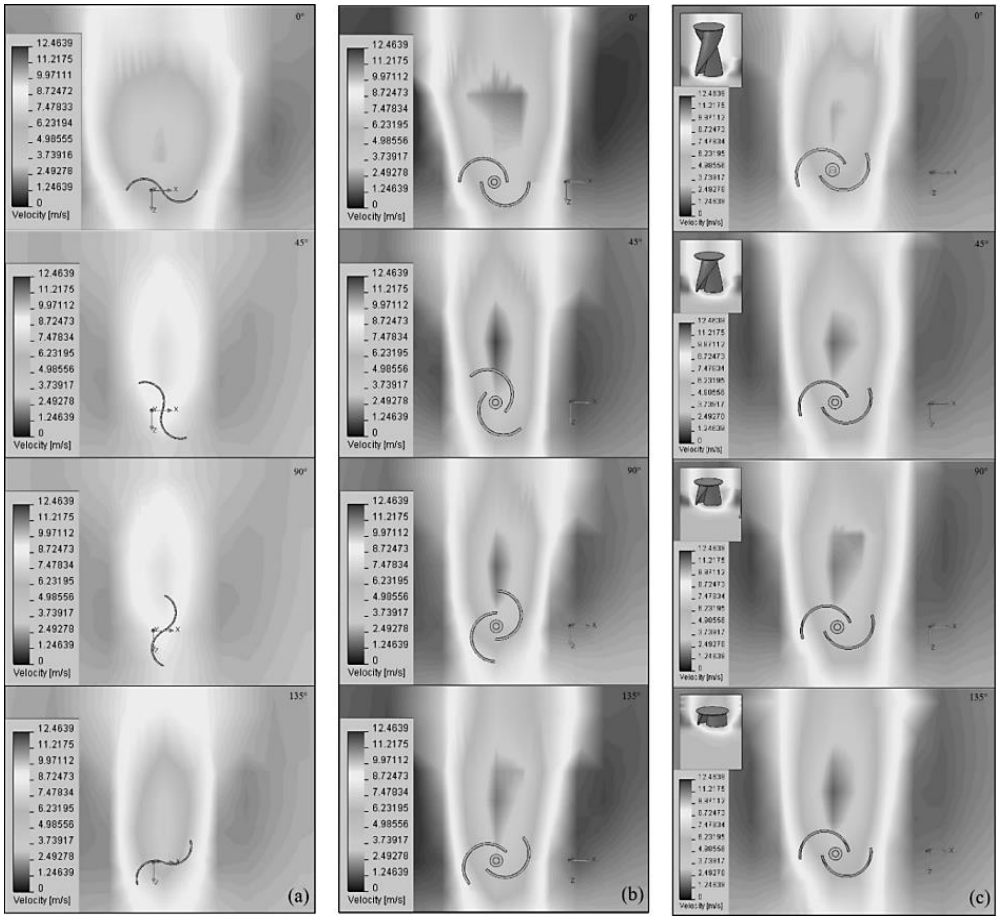

Fig. 7. Incident wind behavior on the Savonius turbines with different positions

The three-dimensional Savonius turbine model without shaft is shown in Fig. 3; Fig. 4 demonstrates the Savonius turbine model with shaft.

Finally, Fig. 5 presents a 3D image of this new proposal. Saha et al. and Hassan et al. have analyzed twisted Savonius turbines [12, 13].

3.1 Our Proposal

Our research uses the profile shown in Fig. 2, this makes a twist that causes a 180° rotation on its own axis; this variation is of great interest because of its specific form which in any position does not stop the wind to impinge on the concave section of the turbine regardless of wind direction.

However, the recruitment section is considerably reduced compared with untwisted Savonius turbines, which have the disadvantage of requiring specific positions in which they give greater wind uptake.

The computational tool used for this analysis is SolidWorks Flow Simulation. Studies in different research areas such as finite element analysis performed by Wang Songtao et al. in [14] as well as W. Tarmizi in their simulation and analysis of the human hand fingers [15] among others [16, 17] support the accuracy of physical development with simulations using SolidWorks utilities.

To perform the following simulations, the software is configured with a total of 1500 flow lines to be able to appreciate the trade wind. It implements a rectangular wind tunnel of 80 x 100

mm with a length of one meter, in which the Savonius turbines are positioned in the middle of the tunnel for testing. The element used is air with an input speed of 10 m/s, with a laminar flow, and a low turbulence of 2%. The end of the tunnel is configured with an environmental pressure of 101325 Pascals at a temperature of 293.2 Kelvin degrees. The material used for the turbines simulation is ABS plastic, due to a low density compared with the density of aluminum and light metal, weighing three grams average per turbine.

In Fig. 6 the performance comparison of the Savonius turbines is shown. The twisted Savonius turbine (Fig. 6c) leads to a reduced residual turbulence.

Fig. 6a shows the wind flow paths incident on the Savonius turbine 3D model without shaft. Fig. 6b illustrates the behavior of the incident wind on the Savonius turbine with shaft, and finally, the same phenomenon on the twisted Savonius turbine can be seen. Obviously, all the turbines are in the same angular position.

4 Obtained Results

Due to the simplicity of the comparison with air flow paths in Fig. 6, Fig. 7 shows a comparison of each turbine behavior with the different air incidence angles. These angles are 0°, 45°, 90°, and, finally, 135°.

The wind incidence at 180° is identical to the incidence at 0°. The Savonius turbines have different positions; Fig. 7 shows the greatest reduction in the air speed passing over the cross section of each turbine. It is important to remark that the turbulence generated by the Savonius turbine without shaft is distributed over approximately 90% of its height. In the case of the twisted Savonius turbine, its turbulence occurs in only approximately 35% of its height. For this reason, the twisted Savonius turbine is proposed for further analysis against the Savonius turbine without shaft, which has a minimal turbulence in 45° and 90° positions.

The Savonius turbine models in 3D were performed with the measures which comply with the relationships mentioned in Section 2. In the case of the Savonius turbine without shaft, its dimensions are shown in Table 3.

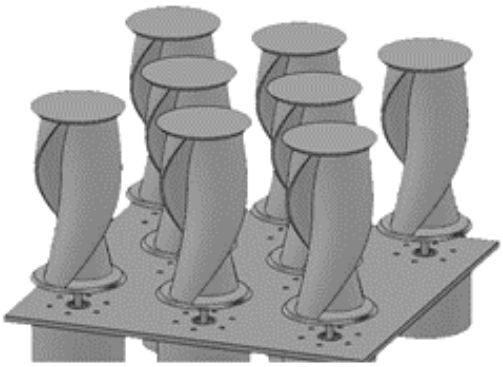

Fig. 8. Module with twisted Savonius micro-turbines

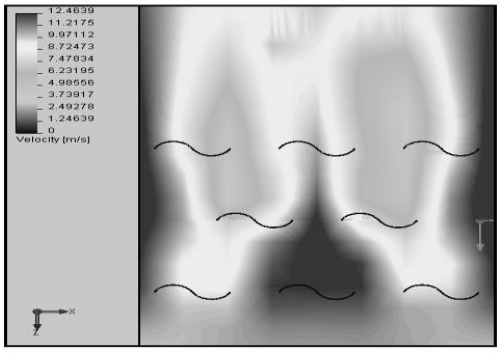

Fig. 9. Behavior of air of the Savonius turbine module without shaft

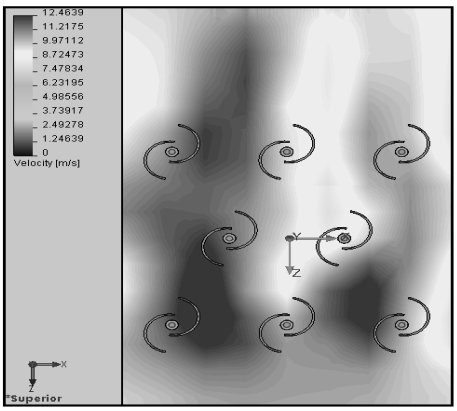

Fig. 10. Behavior of air of the twisted Savonius turbine module

ISSN 2007-9737

Table 3. Analysis of Savonius turbine without shaft

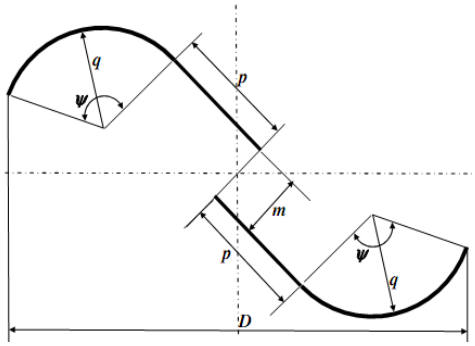

Parameter	*Value*
Turbine Diameter [m]	21.3 mm
Turbine Height [m]	15.9 mm
Blades arc angle [°]	124°
The straight part of each blade [m]	mm
Radius of the arc of the blades [m]	5.7 mm
Plates diameter [m]	25 mm

Table 4. Analysis of the Savonius turbine with shaft

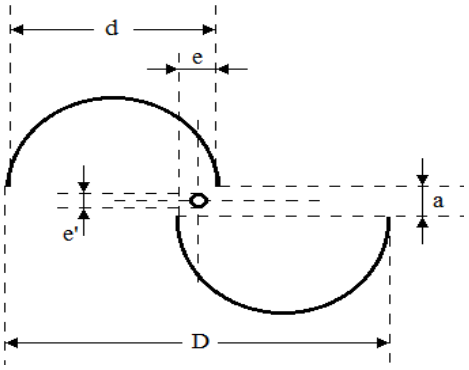

Parameter	*Value*
Turbine Diameter [m]	22.72 mm
Turbine Height [m]	45.45 mm
Blades arc angle [°]	180°
Distance between the blades overlap (m)	7.48 mm
Shaft Diameter [m]	4 mm
Radius of the arc of the blades [m]	14.4 mm
Plates diameter [m]	25 mm

Fig. 7a shows the behavior of the Savonius turbine without shaft, showing the inner dark color only in the positions of 0° and 135° of this turbine, which generates a considerable reduction of the air speed to exit approximately 40 mm after its rotation axis. A similar phenomenon is observed in Fig. 7b, which shows the performance of the Savonius turbine with shaft. However, the latter turbine reduces the air speed at its output in all angular positions analyzed, and in a magnitude of about 80 mm. This is greater than the residual turbulence caused by the Savonius turbine without shaft.

Finally, Fig. 7c shows the behavior of the twisted Savonius turbine which due to its particular form behaves very differently from the other turbines discussed. Although it is turned on its axis, the maximum reduction of the residual air velocity always presents the same profile position. This makes the speed reduction distributed only in a section along the turbine height at its current angular position.

The case of the twisted Savonius turbine meets the same profile as the Savonius turbine with shaft, with only a 180° inclination on its axis. Fig. 8 shows the twisted Savonius turbine module, wherein the position setting is 3 rows of 3, 2 and 3 turbines, respectively. The configuration of this module is proposed in this way to allow the wind to impinge with a higher strength in all the turbines. For the Savonius turbine with shaft, the results are shown in Table 4.

Fig. 9 illustrates the behavior of the incident air speed upon the Savonius turbine module without shaft, which is shown in inner dark with a loss of the incident wind speed of 60% on the last row of turbines. This results in a considerable speed loss of the latter turbines, due to a low wind incident speed.

Fig. 10 depicts the twisted Savonius turbine module behavior, with a maximum loss of 20% in the incident air speed. This can be seen in the tone change from dark gray to white as it slows the air intake from 10 m/s to about 8 m/s on all turbines, which is considerably low compared with losses of 60% of the incident air speed on the Savonius turbines without shaft.

5 Conclusions and Future Work

The twisted Savonius turbine array has presented the best performance with respect to the flow analysis performed. However, from the manufacturing point of view, this type of turbine is the most complex to build, which increases production costs significantly.

Once this module manufacture is carried out, a new analysis is suggested focusing on power generation using modular commercial micro-motors as power generators. The object of this proposal is to implement Savonius turbine arrays on buildings at low cost. An array of eight TST for a continuous energy generator system where other wind systems are not viable is proposed.

So far, as in the case of buildings it is not always possible to use traditional wind generators; using arrays of twisted Savonius micro-turbines combined with solar cells would be a feasible option. The above could be used for fuel consumption reduction and, consequently, a reduction in greenhouse gas emissions.

Acknowledgements

This work has been funded by Instituto Politécnico Nacional.

References

1. **Chang, L. (2002).** Wind Energy Conversion System. *IEEE Canadian Review*, pp. 12–16.
2. **Sargolzaei, J. (2007).** Prediction of the Power Ratio in Wind Turbine Savonius Rotors Using Artificial Neural Networks. *International Journal of Energy and Environment*, Vol. 1, No. 2, pp. 51–55.
3. **Sargolzaei, J. & Kianifar, A. (2010).** Neuro-fuzzy modeling *tools* for estimation of torque in Savonius rotor wind turbine. *Advances in Engineering Software*, Vol. 41, No. 4, pp. 619–626, doi: 10.1016/j.advengsoft.2009.12.002.
4. **Eriksson, S., Bernhoff, H. & Leijon, M. (2006).** Evaluation of different turbine concepts for wind power. *Renewable and Sustainable Energy Reviews*, Vol. 12, No. 5, pp. 1419–1434, doi: 10.1016/j.rser.2006.05.017.
5. **Sargolzaei, J. & Kianifar, A. (2009).** Modeling and simulation of wind turbine Savonius rotors using artificial neural networks for estimation of the power ratio and torque. *Simulation Modeling Practice and Theory*, Vol. 17, No. 7, pp. 1290–1298. doi: 10.1016/j.simpat.2009.05.003.
6. **Kamoji, M.A., Kedare, S., & Prabhu, S. (2008).** Experimental investigations on single stage *modified* Savonius rotor. *Applied Energy*, Vol. 86, No. 7-8, pp. 1064–107, doi: 10.1016/j.apenergy.2008.09.019.
7. **Savonious, S.J. (1931).** The S-rotor and its application. *Mechanical Engineering*, Vol. 53, No. 5, pp. 333–338.
8. **Hayashi, T., Li, Y., Hara, Y., & Suzuki, K. (2005).** Wind tunnel tests on a three-stage out-phase Savonius rotor. *JSME International Journal* , Vol. 48, No. 1, pp. 9–16.
9. **Menet, J. & Bourabaa, N. (2004).** Increase in the Savonious rotors efficiency via a parametric investigation. *Proc. of European wind energy*, London, U.K.
10. **Nakajima, M., Lio, S., & Ikeda, T. (2008).** Performance of Savonius rotor for *environmentally* friendly hydraulic turbine. *Journal of Fluid Science and Technology,* Vol. 3, No. 3, pp. 420–429, doi: 10.1299/jfst.3.420.
11. **Nakajima, M., Lio, S., & Ikeda, T. (2008).** Performance of Double-step Savonius Rotor for Environmentally Friendly Hydraulic Turbine. *Journal of Fluid Science and Technology*, Vol. 3, No. 3, pp. 410–419.
12. **Saha, U.K. & Rajkumar, M. (2006).** On the performance analysis of Savonius rotor with twisted blades. *Renewable Energy*, Vol. 31, No. 11, pp. 1776–1788, doi: 10.1016/j.renene.2005.08.030.
13. **Hassan, M., Iqbal, T., Khan, N., Hinchey, M., & Masek, V. (2010).** CFD Analysis of a Twisted Savonius Turbine. *Proc. of NECEC*, St. John's, Newfoundland, Canada.
14. **Wang, S. & Li, A. (2010).** Parameterizedly Design Cam Based on Excel and SolidWorks and Finite element analysis and Simulation by COSMOS. *E-Product E-Service and E-Entertainment (ICEEE)*, doi: 10.1109/ICEEE.2010.5660856.
15. **Tarmizi, W. & Faizura, W. (2010).** Modeling and Simulation of a Multi-Fingered Robot Hand. *International Conference on Intelligent and Advanced Systems* (ICIAS 2010), pp. 15–17, Kuala Lumpur, Malaysia, doi: 10.1109/ICIAS.2010.5716220.
16. **Hira, K. & Levent, M. (2009).** Design of Medical Robotic Operating Rooms by SolidWorks. *Biomedical Engineering* Meeting *(BIYOMUT 2009),* doi: 10.1109/BIYOMUT.2009.5130327.

17. Fuqin, Y., Hao, C., & Degong, C. (2009). Kinematic Simulation of a Spatial Staggered Joint Based on COSMOS Motion. *Intelligent Human-Machine Systems and Cybernetics (IHMSC'09),* doi: 10.1109/IHMSC.2009.233.

18. The Royal Academy of Engineering (2008). *Wind Turbine Power Calculations*.

Jesús Antonio Alvarez-Cedillo is an engineer graduated from Instituto Politécnico Nacional (1987). He received the M.Sc. in Computer Science (2002) from CINTEC-IPN, Mexico. Currently, he is pursuing the Ph.D. with CIDETEC-IPN. His areas of interests are computer architectures, parallel and distributed architectures, operating systems for parallel and distributed systems, graphing modeling, and town memory GPUs.

Mauricio Olguín-Carbajal received his Ph.D. in Computer Sciences from CIC-IPN, Mexico, in 2011. He worked with power generation dedicated systems in electrical industry until 2002 implementing communication protocols for SCADA systems. Since 2005 he has been a researcher in CIDETEC-IPN. His mayor research areas are computer 3D modeling and simulation, computer graphics, virtual reality, networking, and network security.

Juan Carlos Herrera-Lozada received the Ph.D. in Computer Science and the M.Sc. in Computer Engineering from Centro de Investigacion en Computación (CIC) of the Instituto Politecnico Nacional (IPN), in Mexico City. He has authored several articles and has been a speaker at national and international conferences. He has participated in different research projects and technological developments. His research interests include design of reconfigurable logic devices, practical applications with microcontrollers, and embedded systems design.

Ramón Silva-Ortigoza received his Ph.D. in Electrical Engineering (Mechatronics) from CINVESTAV-IPN, in 2006. Currently Dr. Silva is a member of the Mexican National System of Researchers (SNI) and works in CIDETEC-IPN, Mexico. He is co-author of the book *Control Design Techniques in Power Electronics Devices* (Springer-Verlag, London, 2006). His areas of interests are mechatronical control systems, mobile robotic, and design of control techniques applied to electronic control power systems.

Jacobo Sandoval-Gutiérrez received his Master degree and his Ph.D. in Advanced Technology from CICATA-IPN, in 2006 and 2010, respectively. His areas of interests are computer architectures, parallel computing, 3D manufacturing, and robotics. He has co-authored articles and patents in multidisciplinary topics.

Article received on 14/05/2014; accepted on 14/01/2015.
Corresponding author is Jesús Antonio Alvarez-Cedillo.